Chapter 12

Mediated Surface Properties of Polybenzoxazines

M.G. Mohamed*, R.-C. Lin*, K.-C. Hsu*, W. Zhang†, X. Zhong† and S.-W. Kuo*,[1]

*National Sun Yat-Sen University, Kaohsiung, Taiwan, †East China University of Science and Technology, Shanghai, China

[1]Corresponding author: e-mail: kuosw@faculty.nsysu.edu.tw

Chapter Outline

1 INTRODUCTION

Mediated surface properties are able to evaluate the performance of polymer materials, including wettability, adhesion, and friction. For instance, the low-surface-free energy of polymer materials plays an important role for biomedical layers, sports, outdoor clothing, and environmental fouling applications [1–5]. We usually use the fluorine- or silicon-containing polymers to prepare the low-surface-free-energy property [6–9] and the benchmark of low surface energy material of polymer materials is the poly(tetrafluoroethylene) (PTFE) because of its ability to repel water [6,10,11]. However, PTFE and other fluorinated polymers possess their limitations because of their high cost and poor processability in industrial applications and thus the new low-surface-free-energy polymeric materials without fluorine compound are quite important for further application in surface engineering [12–26].

It is generally believed that the physical crosslinking interactions between polybenzoxazine polymer chains that take place through intermolecular or intramolecular hydrogen bonding interaction play an important role in surface properties of polymers. For example, Chung et al. reported that incorporating the amide groups into the fluorinated main chain liquid crystalline polymer was prepared through thin film polymerization. They found that an amide group (NHCO) is able to induce strong intermolecular hydrogen interaction, which leads to a high surface free energy and low water contact angle (WCA) [27].

The Jiang group found that strong intramolecular hydrogen bonding interaction of PNIPAAm between the N—H and C═O groups shows the hydrophobic property of PNIPAAm of its collapsed conformation results when the temperature is higher than its lower critical solution temperature [28]. We realize that the surface free energy is strongly dependent on the intermolecular interaction when increasing of intramolecular hydrogen bonds of polymer chain is able to decrease the surface free energy based on these previous studies [27,28].

2 SURFACE PROPERTIES OF POLYBENZOXAZINES

2.1 Low-Surface-Free-Energy Materials Based on Polybenzoxazines

Low-surface-free-energy materials have attracted the attention of the academic and industrial communities because of their possible applications in biomaterials and coating. Polybenzoxazines are novel thermosetting polymers with unique physical properties [29], and their properties are influenced by the strong intramolecular hydrogen bonding interactions as well as intermolecular hydrogen bonding between polybenzoxazine polymer chains [30]. There are many methods to generate low-surface-free-energy materials involving self-assembly [31], electrospinning [32], sol–gel solution [33], and chemical etching [34].

Advanced and Emerging Polybenzoxazine Science and Technology. http://dx.doi.org/10.1016/B978-0-12-804170-3.00012-3

In 2006, Wang et al. supposed that polybenzoxazine possessed the low-surface-free-energy property because of its strong intramolecular hydrogen bonding interaction between the OH group and N-atom of polybenzoxazine without fluorine and silicon atoms [35]. Based on the FTIR spectra, the fraction of −OH···N intramolecular hydrogen bonds (ca.3120–3170 cm^{-1}) is very important to determine the surface free energy property and the surface free energy of 2,2-bis(3,4-dihydro-3-methyl-2*H*-1,3-benzoxazine) propane (BA-m) and 2,2-bis(3,4-dihydro-3-phenyl-2*H*-1,3-benzoxazine) propane (BA-a) are 16.4 and 19.2 mJ/m^2, respectively, because of their different fractions of −OH···N intramolecular hydrogen bonds. In addition, Qu et al. synthesized TFP-tmos monomer through Mannich condensation of 4-trifluoremethylphenol, 3-aminopropyltrimethoxysilane, and formaldehyde solution and the film of poly(TFP-tmos) also displayed a low-surface-free energy (15.50 mJ/m^2) [36].

Recently, Xin et al. prepared a new low-surface-free energy of polybenzoxazines films based on silane group as shown in Scheme 1 [37]. In this report, the surface free energy (y_s) of polybenzoxazine film was investigated by using Owen's three ligand method. The surface free energy of poly(3-(trimethoxysilyl)-*n*-propyl-3,4-dihydro-2*H*-1,3-benzoxazine) (P-tmos), poly(3-(trimethoxysilyl)-*n*-propyl-3,4-dihydro-6-methyl-2*H*-1,3-benzoxazine) (MP-tmos), and poly(3-(trimethoxysilyl)-*n*-propyl-3,4-dihydro-6-*tert*-butyl-2*H*-1,3-benzoxazine) (PTBP-tmos) after thermal curing polymerization at 200°C were 15.64, 14.91, and 14.93 mJ/m^2.

In 2013, Chang et al. prepared the 3-phenyl-3,4-dihydro-2*H*-1,3-benzoxazine (P-a) and then blended with polyacrylonitrile (PAN) to obtain low-surface-free-energy materials without fluorine as shown in Scheme 2 [38]. FTIR results showed that the intermolecular interaction existed between phenolic hydroxyl group of poly(P-a)s after the ring opening reaction with cyano group in PAN to afford heteroaromatic cyclic structure after polymerization at 300°C.

The WCA of PAN/(P-a) and PAN/poly(P-a) blends were measured after preparing samples by spin coating and electrospinning methods as shown in Fig. 1. The WCA values of PAN fibers prepared by electrospinning was much higher (104 degree ± 3 degree) than that of PAN fibers by spin

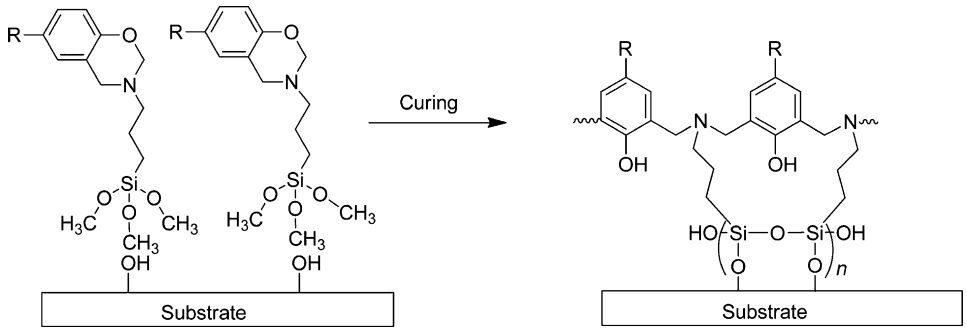

SCHEME 1 Schematic diagram illustrating the process of poly(TFP-tmos) film formation [37].

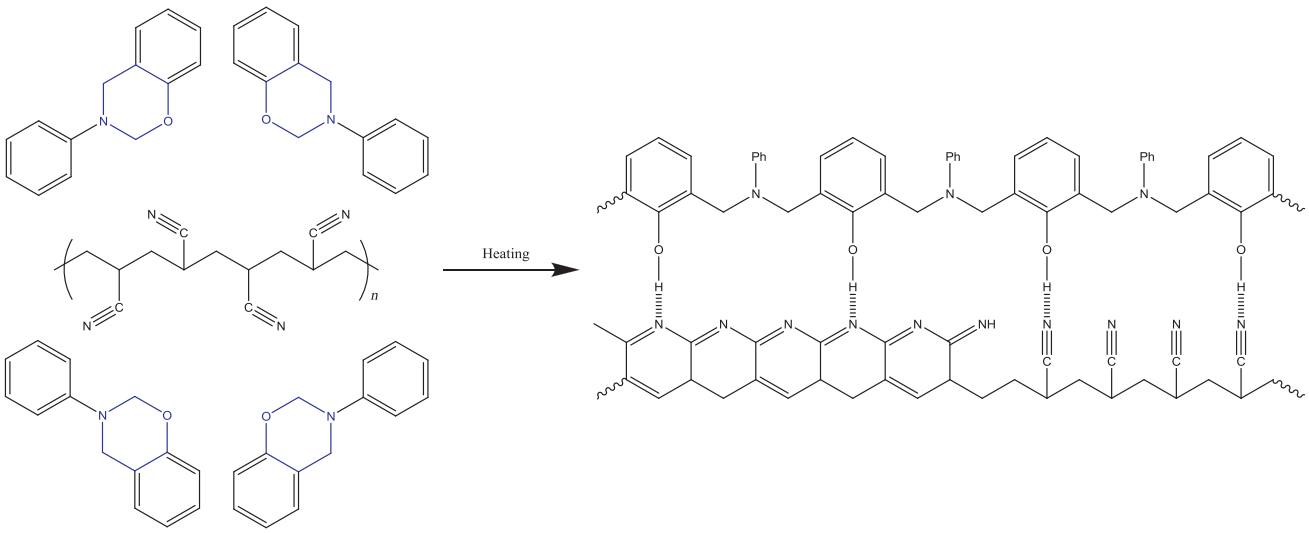

SCHEME 2 Intermolecular hydrogen bonding between hydroxyl groups of poly(P-a) chains and heteroaromatic or polyimine cyclic group in the PAN after curing PAN/(P-a) hybrids [38].

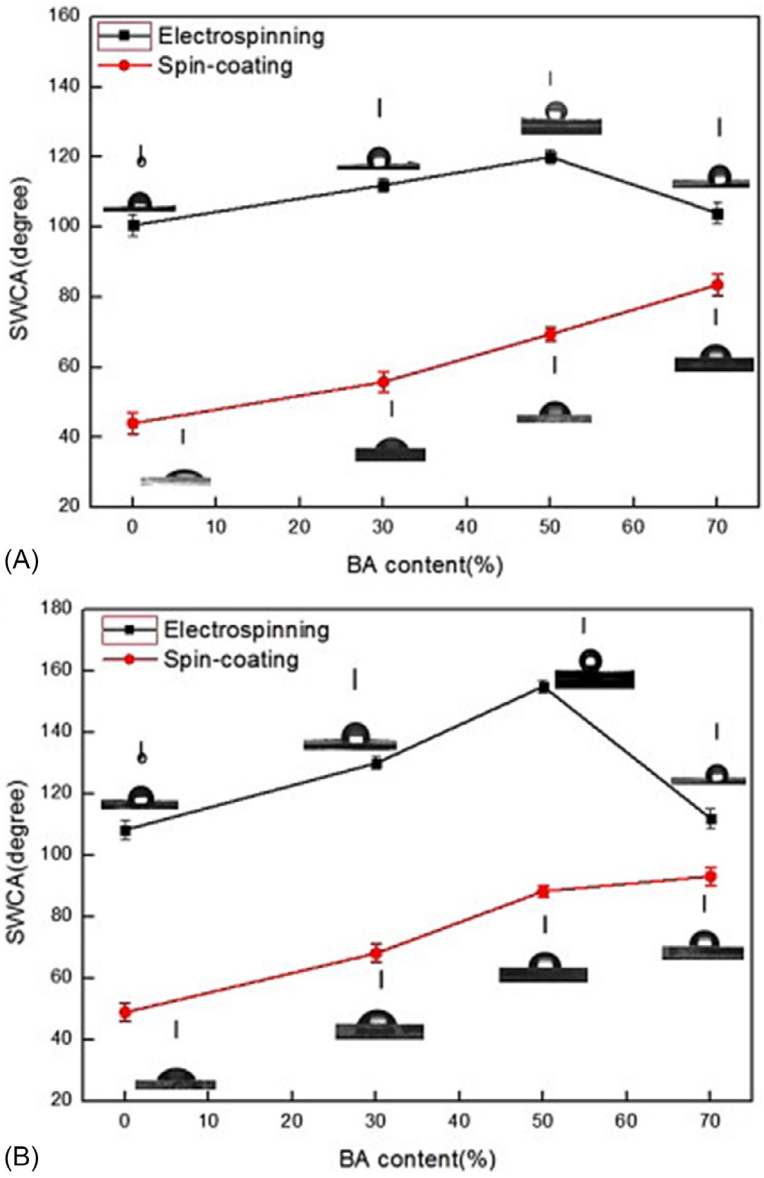

FIG. 1 Dependence of static water contact angle (SWCA) of (A) PAN/(P-a) hybrids and (B) PAN/poly(P-a) blends prepared by spin coating and electrospinning on the surface upon increase of P-a monomer content [38].

coating approach (44 degree ± 3 degree). After increasing the P-a monomer contents to 50 wt%, the WCAs of PAN fibers prepared by electrospinning method gradually increased to (120 degree ± 3 degree). After increasing the curing temperature of PAN/(P-a) blends, the WCAs of PAN/poly(P-a) prepared through electrospinning increased to 154 degree ± 3 degree. This value indicates that the surface properties became superhydrophobic because of the structural change of the polymer PAN/poly(P-a) fibrous mats and nature surface chemistry property.

We also reported that a novel class of poly(OPOSS-pa) nanocomposites was synthesized from octa-azido functionalized polyhedral oligomeric silsesquioxane ($OVBN_3$-POSS) with 3,4-dihydro-3-(prop-2-ynyl)-2*H*-benzooxazine (P-pa) monomer via the click reaction. It showed a network of structures through thermal curing of multifunctional benzoxazine groups of POSS. We found that the surface free energy of poly(OPOSS-pa) (14.6 mJ/m^2) is lower than that of PTFE (22 mJ/m^2) [39,40]. The CAs of modified poly(4-vinylpyridine) thin film with poly(OPOSS-pa) showed the highest contact angle (CA) values in water, followed by diiodomethane and ethylene glycol (105 degree, 78.1 degree, and 97.3 degree), which are all expectedly higher than unmodified poly(4-vinylpyridine) thin film as shown in Fig. 2.

2.2 Durable Resistance Applications of Polybenzoxazines

As we mentioned above, polybenzoxazine is a new low-surface-free-energy material with 16.4 mJ/m^2 and can be used in nanoimprint lithography (NIL) because of its

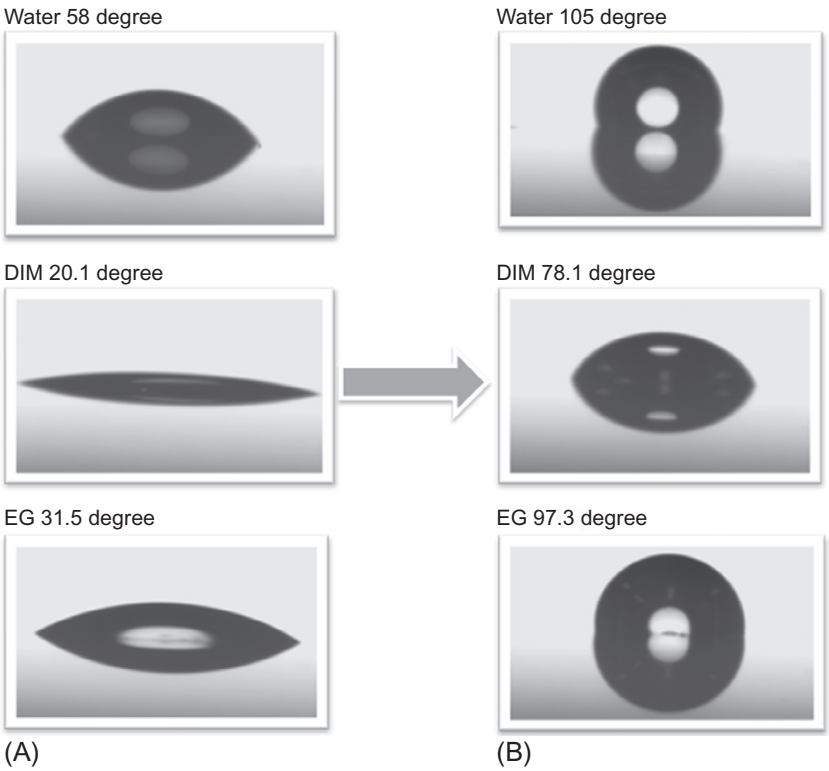

FIG. 2 The advancing contact angle for waters, ethylene glycol (EG), and diiodomethane (DIM) of (A) poly(4-vinylpyridine) thin film (B) modified with poly(OPOSS-pa) thin film [40].

mold-release capability without any side reaction, the use of inexpensive materials, and ease of fabrication. Generally, there are two ways to achieve NIL, a next-generation lithography: hot-embossing by using thermosetting polymers (E-NIL) and a UV-based NIL by using UV-curable polymer system (UV-NIL). The NIL process is strongly dependent on the adhesion characteristic between the resist polymer and mold. In 2007, Wang et al. used poly(BA-m) as a mold-release agent for NIL, and showed that polybenzoxazine, after treated with mold, self-cleaned after imprinting 13 times, according to atomic force microscope (AFM) images as shown in Fig. 3 [41]. In 2013, Wang et al. synthesized BA-aa through Mannich condensation of bisphenol A and allylamine and paraformaldehyde, and fabricated poly(BA-aa) with patterned nickel stamp by roller NIL approach using an ultraviolet-curable resin [42]. They found that the contact angle and surface free energy of poly(BA-aa) mold was much smaller than that nickel mold.

2.3 Tuning the Surface Properties of Polybenzoxazines Thin Film

Thermal polymerization of benzoxazine monomer to give polybenzoxazine thermosetting polymers with highly physical crosslinking density through strong intramolecular

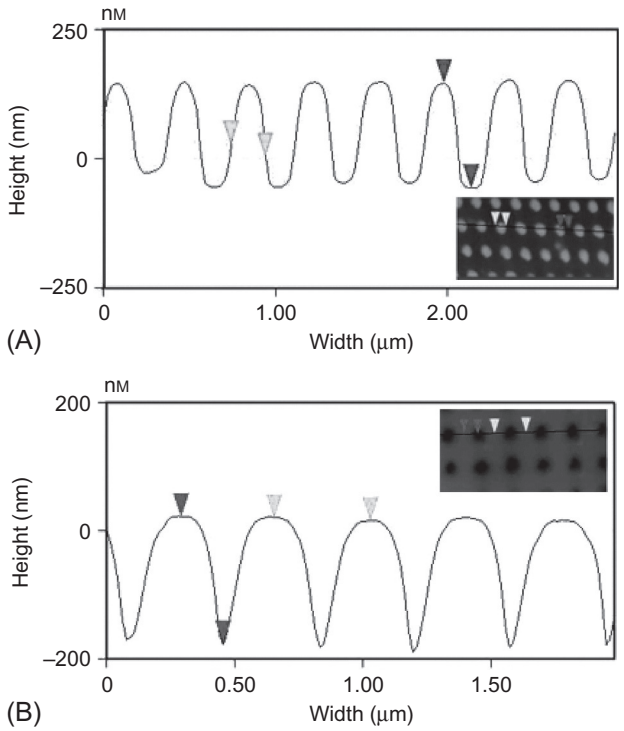

FIG. 3 AFM images of (A) the poly(BA-m) treated mold (cylinders) after imprinting 13 times. (B) Resist pattern (holes) on the substrate after imprinting with poly(BA-m) treated mold [41].

hydrogen bonding between the OH groups and the N-atoms in the Mannich base bridge results in reducing surface free energy, while intermolecular hydrogen bonding between phenolic groups itself tends to increase the surface free energy for polybenzoxazines system.

Many methods are applied to tune the surface and interfacial characteristics of polybenzoxazine from hydrophobic to hydrophilic surfaces, including ultraviolet thermal treatment [43], acidification method [44], light irradiation such as azobenzene units [45,46], TiO_2 [47], and electrical current [48,49]. Recently, we designed and synthesized three different types of functionalized polybenzoxazines carrying azobenzene as photoresponsive moiety, and their surface properties can be tuned upon photoirradiation at 365 nm.

For instance, we synthesized polymerized azopyridine functionalized benzoxazine (AZOPY-a) as shown in Scheme 3 [50]. The UV-vis profile shows that trans isomer of AZOPY-a has an absorption peak at 360 nm which corresponds to the π-π* transition. After UV irradiation of the trans isomer at 365 nm at different times (1–5 min), the maximum absorption band of the trans isomer decreased and shifted to lower wavelength (333 nm), which ascribed to the cis isomer of AZOPY-a. In addition, the cis isomer of AZOPY-a shifted back to the original absorption band frequency at 360 nm upon irradiation under UV light at 443 nm as displayed in Fig. 4. Fig. 5 displays that the WCA value of the trans isomer AZOPY-a (89 degree) was higher than that cis isomer (29 degree) at room temperature because planar trans isomer has a smaller dipole moment and low-surface-free energy. Further increase in polymerization temperature to 150°C, both trans and cis isomers of poly(AZOPY-a) showed a similar WCA value

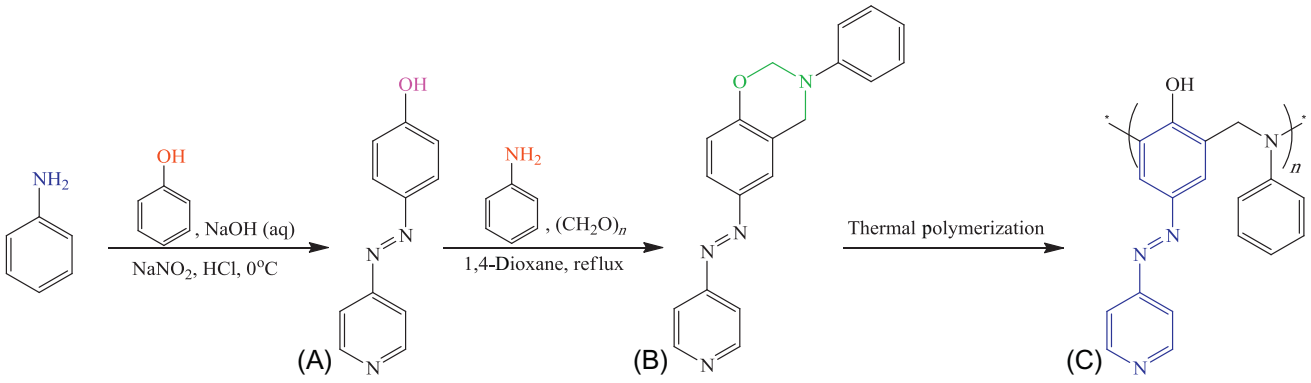

SCHEME 3 Synthesis of (A) AzoPy-OH, (B) AZOPY-a, and (C) poly(AZOPY-a) [50].

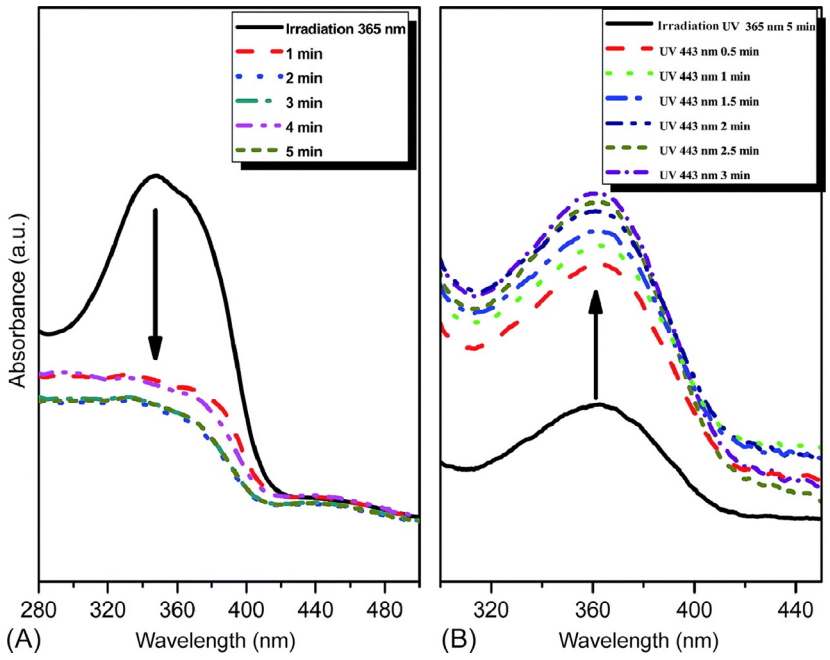

FIG. 4 UV-vis absorption of AZOPY-a (10^{-4} M in THF) (A) before and (B) after irradiation with UV light at 365 nm for different periods of time [50].

of 101 degree due to strong intramolecular hydrogen bonding after opening the benzoxazine ring.

We also used hydrogen bonding approach as noncovalent interaction between the azo-COOH functionalized benzoxazine (AZOCOOH-a) and AZOPY-a to form a supramolecular complex as presented in Scheme 4 [51]. It shows that the WCA value of *trans* AZOCOOH-a is much higher than *cis* AZOCOOH-a because of the presence of strong intermolecular hydrogen bonds of carboxyl (COOH) groups, while the WCA value of AZOCOOH-a/AZOPY-a supramolecular complex was smaller than that of the pure *trans* AZOCOOH-a before and after thermal polymerization from 25°C to 150°C, which is believed to have increased the surface free energy through intermolecular hydrogen bonding and decreasing the hydrophobicity of the surface. After thermal curing in the range between 180°C and 210°C, the poly

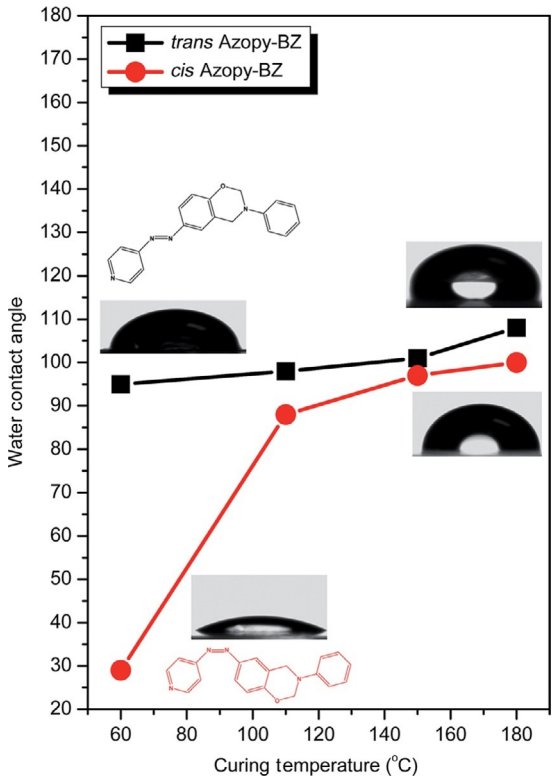

FIG. 5 Water contact angle (WCA) of AZOPY-a in its trans and cis isomeric forms, recorded after each stage [50].

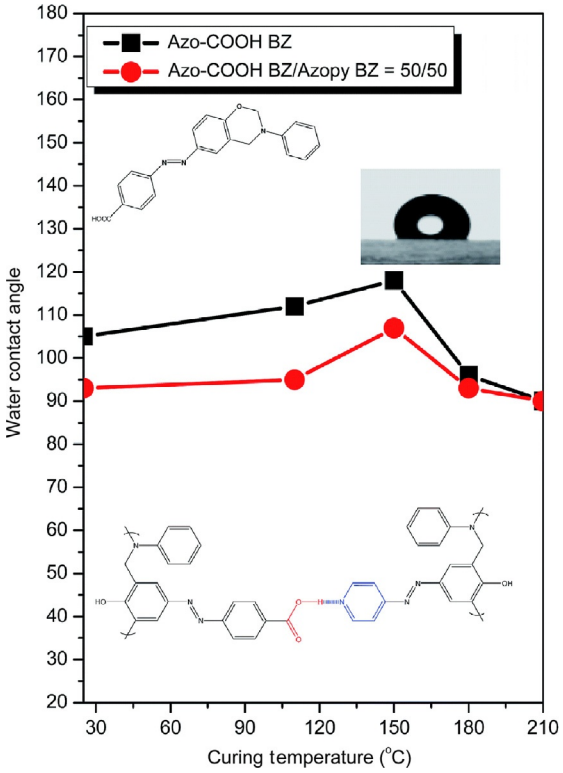

FIG. 6 Water contact angles (WCA) of AZOCOOH-a/AZOPY-a = 50/50 supramolecular complex in its trans and cis isomeric forms, recorded after each curing stage [51].

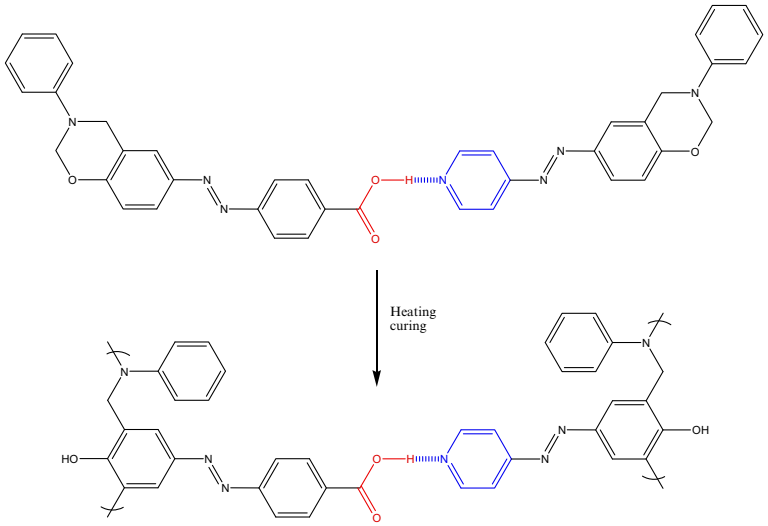

SCHEME 4 Hydrogen bonding between AZOCOOH-a and AZOPY-a monomers and in their corresponding polymer blends [51].

(AZOCOOH-a) and poly(AZOCOOH-a)/poly(AZOPY-a) supramolecular complex have a similar WCA values (Fig. 6).

We also designed multifunctional polybenzoxazine containing azobenzene units, COOH groups and pyrene moiety (AZOCOOH-py) and shown in Scheme 5 [52]. This system showed tunable surface properties from hydrophilic surface (the trans isomer) to hydrophobic surface (the cis isomer) at ambient temperature. The WCA was still higher upon increasing the thermal curing than those of uncured AZOCOOH-py because of the formation of the network structure after the opening of the benzoxazine monomer through six membered rings between phenolic hydroxyl groups with Mannich base bridge.

In 2013, we reported a simple approach for reversible surface of a poly(BA-aa) thin film through UV illumination and thermal treatment (Scheme 6) [53]. Fig. 7 shows that the WCAs of poly(BA-aa) increased from 81 degree to 103 degree upon polymerization temperature at 200°C, and WCAs decreased to 0 degree after UV exposure because of increasing the degree of intermolecular interaction, thereby the surface was tuned from hydrophobic to superhydrophilic. Interestingly, the WCAs came back to the original

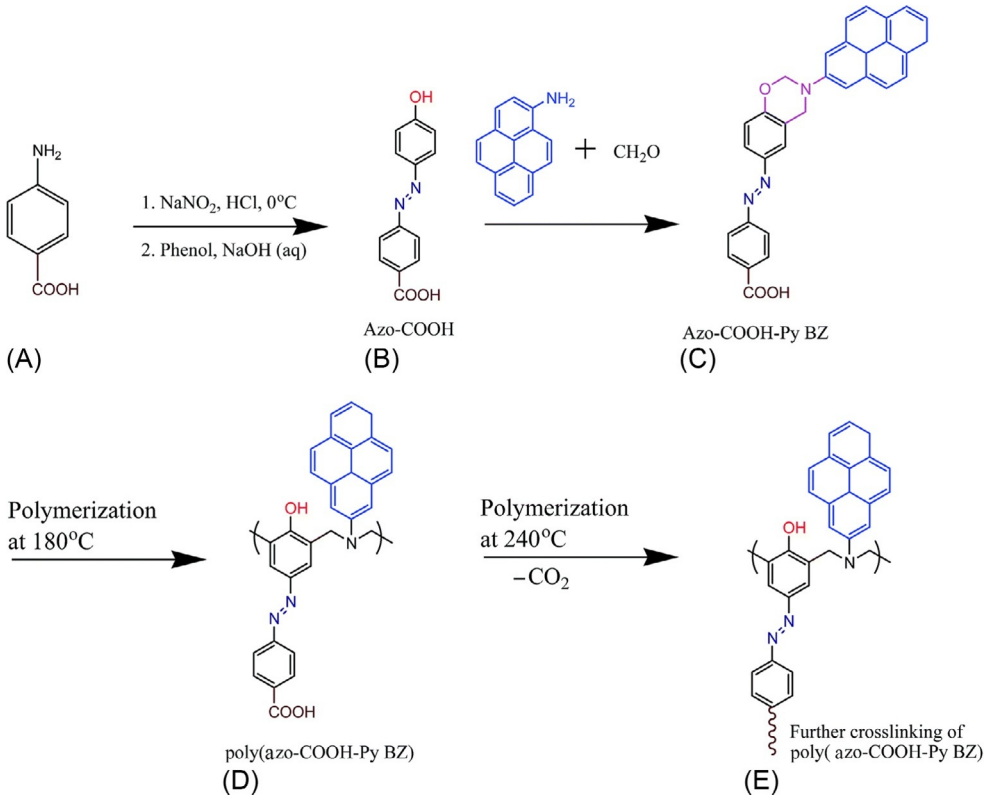

SCHEME 5 (A) 4-Aminobenzoic acid and synthesis of (B) Azo-COOH, (C) AZOCOOH-py, (D) poly(AzoCOOH-Py), and (E) further crosslinking of poly(AZOCOOH-py) after curing at 240°C [52].

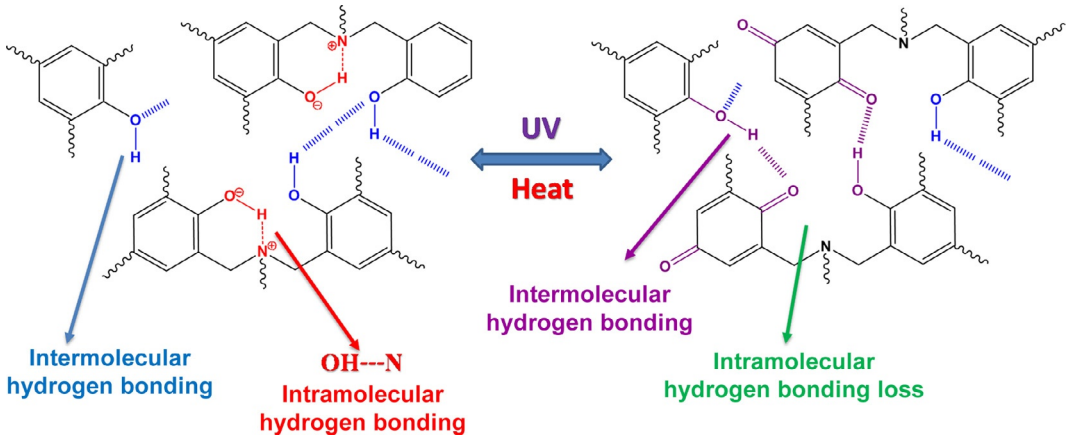

SCHEME 6 Possible reversible BA-aa chemical structures formed upon alternating UV irradiation and thermal treatment [53].

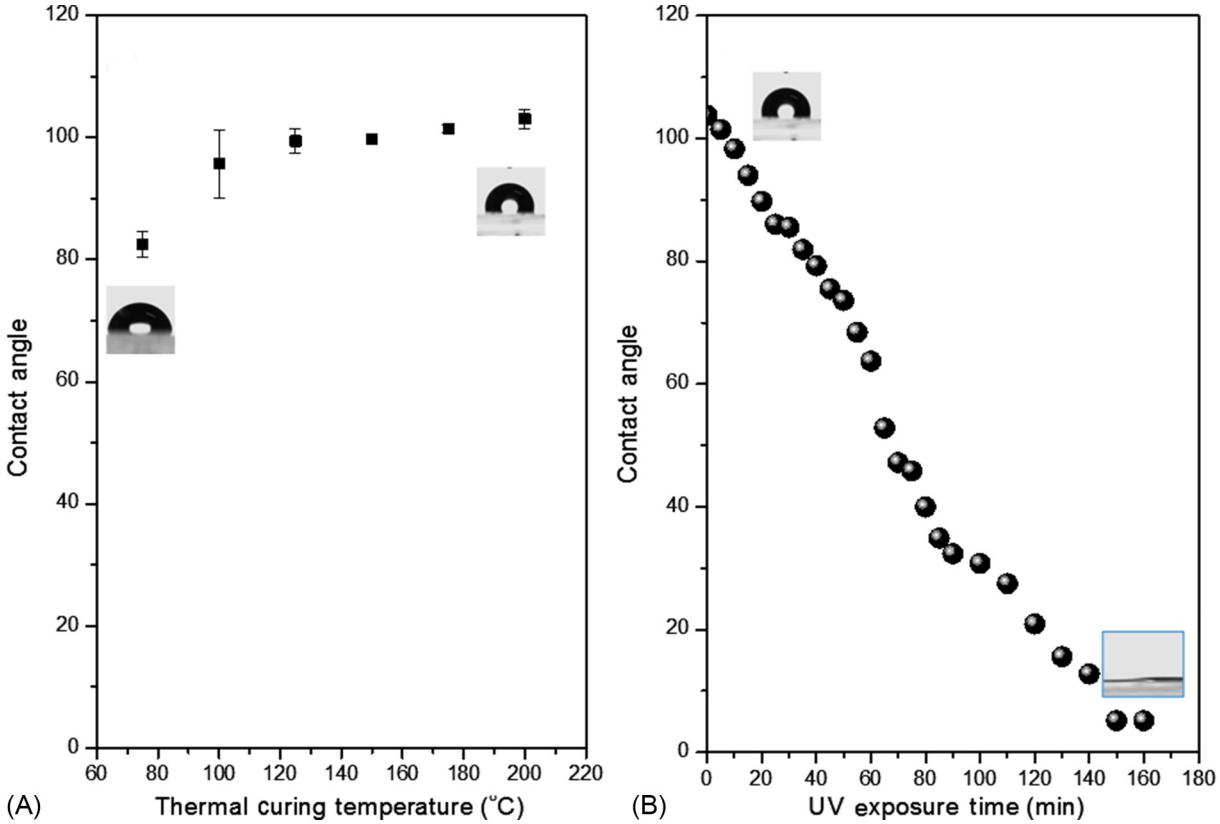

FIG. 7 Variation in WCA after (A) the first thermal curing of the BA-aa monomer at various temperatures and (B) the first UV exposure for various lengths of time [53].

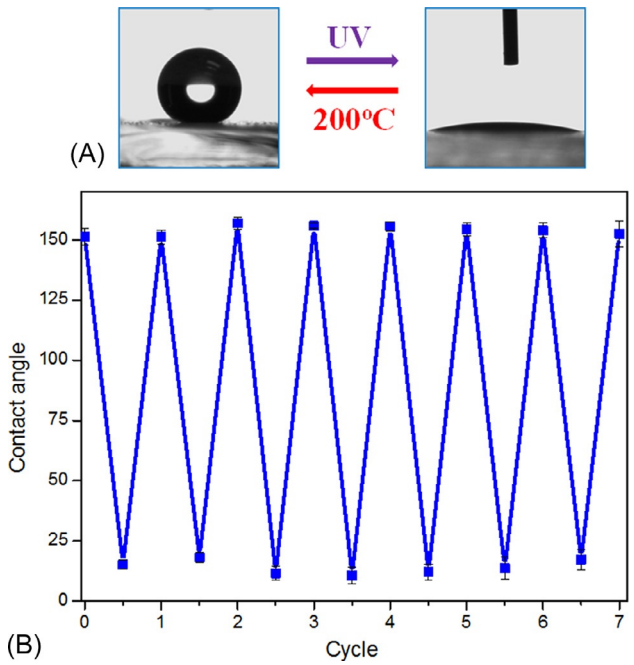

FIG. 8 (A) Photographs of a water droplet on the poly(BA-aa)/silica hybrid surface modified with a poly(BA-aa) coating before (left) and after (right) UV illumination. (B) Reversible superhydrophobic-superhydrophilic transitions of the as-prepared coating upon sequential alternating of UV irradiation and thermal treatment [53].

value of cured poly(BA-aa) at 200°C after second thermal treatment of UV-exposed poly(BA-aa) (Fig. 8).

Without any fluorine-containing surface modification agent, Zhang et al. reported a superhydrophobic silane-functionalized polybenzoxazine of poly(MP-tmos)/TiO_2 nanocomposites film with a large WCA of c.166 degree [47]. The pure polybenzoxazine film had no obvious photoresponsive property under the 10-h irradiation and maintained its hydrophobicity, indicating an antiUV property of poly (MP-tmos). However, the content of TiO_2 affects reversibly switchable wettability of poly(MP-tmos)/TiO_2 film. When the mass percentage of TiO_2 to benzoxazine monomer was increased to 60%, the consequent nanocomposite film enjoyed superhydrophobicity-superhydrophilicity conversions with a variation of around 125 degree in WCA upon UV exposure-heat treatment cycles (Fig. 9A). The photo-induced superhydrophilicity occurs because of an increasing content of Ti-OH on the surface of poly(MP-tmos)/TiO_2 film (Fig. 9B). When irradiated by UV light, TiO_2 generated electrons and holes. The photo-generated hole reacted with lattice oxygen to form surface oxygen vacancy. Then water molecules (hydroxyl) were absorbed into the oxygen vacancy leading to water adsorption on the surface, transforming the originally hydrophobic poly(MP-tmos)/TiO_2 surface into superhydrophilic. On the contrary, hydroxyl groups were replaced gradually

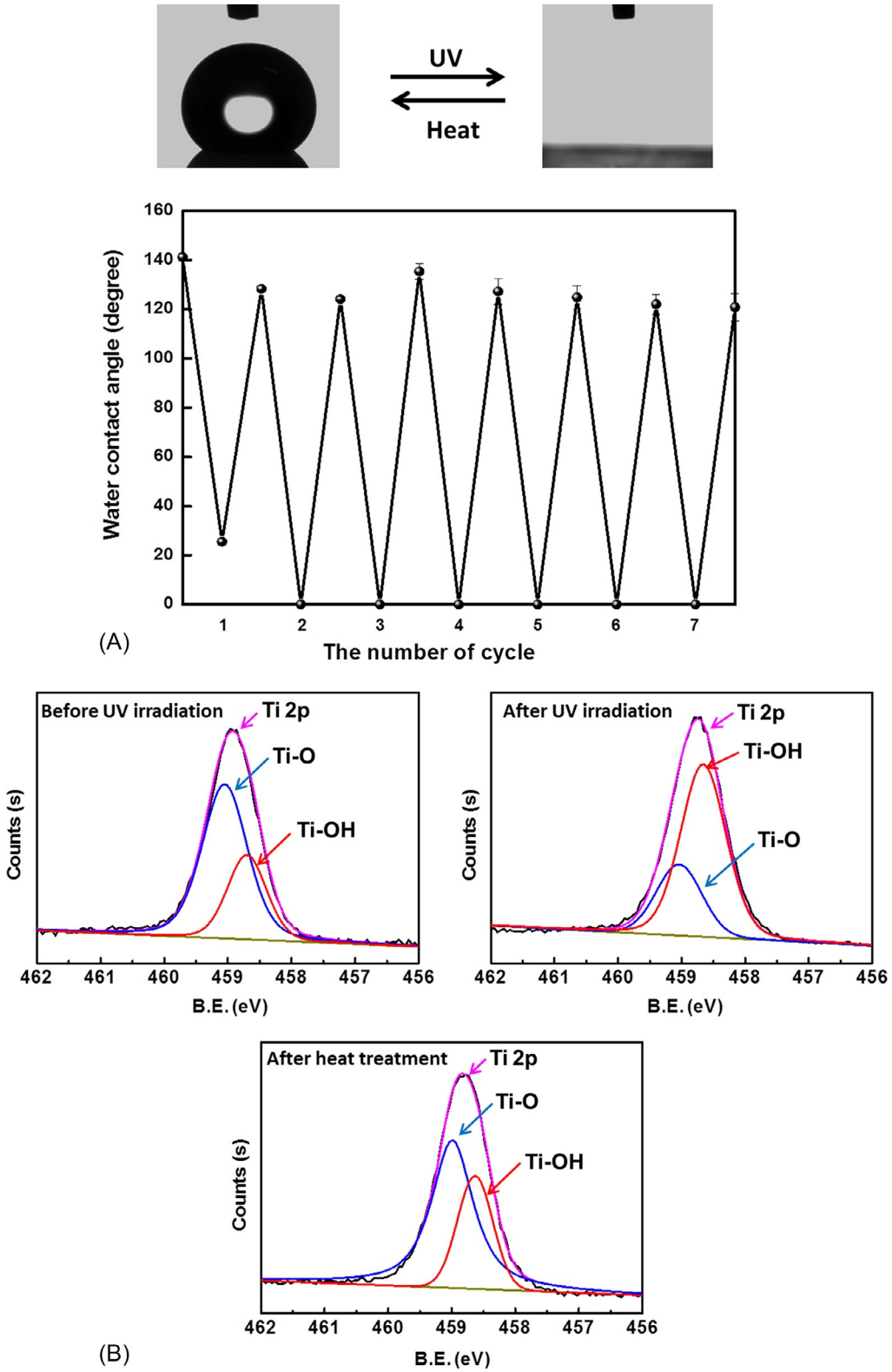

FIG. 9 (A) Reversible hydrophobic-superhydrophilic transitions of poly(MP-tmos)/TiO_2 film through UV exposure-heat treatment cycles, and (B) XPS spectra (Ti 2p peaks) of poly(MP-tmos)/TiO_2 film before and after UV irradiation and after heat treatment (the weight ratio of TiO_2/MP-tmos = 60% for all hybrid films) [47].

by atmospheric oxygen when exposing poly(MP-tmos)/TiO_2 to heat, thus resulting in a hydrophobic surface.

2.4 Superhydrophobic Surfaces

Superhydrophobic surface (water repellent) materials are materials that possess a WCA greater than 150 degree and have potential applications in liquid transportation, microfluidics system, drag reduction, and self-cleaning materials [54–57]. In order to achieve the superhydrophobic surfaces, many methods, such as NIL, etching, plasma treatment, and chemical fabrication of a rough surface by incorporating low surface species into the rough substrate, are employed. It is desirable to prepare superhydrophobic films by inexpensive materials and easier fabrication process. Wenzel and Cassie offered two different theoretical models that propose to explain the increasing surface roughness leading to higher WCA [58,59]. In 2006, Chang et al. have successfully achieved the preparation of the superhydrophobic surface films of poly(BA-aa) and poly(BA-m) by a two-casting method with equivalent content of SiO_2 [60,61].

2.4.1 *Polybenzoxazine/SiO_2 Hybrid Superhydrophobic Surfaces*

In 2012, Ding et al. fabricated superhydrophobic silica nanofibrous membranes through in situ polymerization of a bifunctional fluorinated benzoxazine, 2,2-bis(3-*m*-trifluoromethylphenyl-3,4-dihydro-2*H*-1,3-benzoxazinyl) propane (BAF-tfa) with SiO_2 nanoparticles (SNPs) on electrospun silica nanofibers as shown in Scheme 7 [62]. The

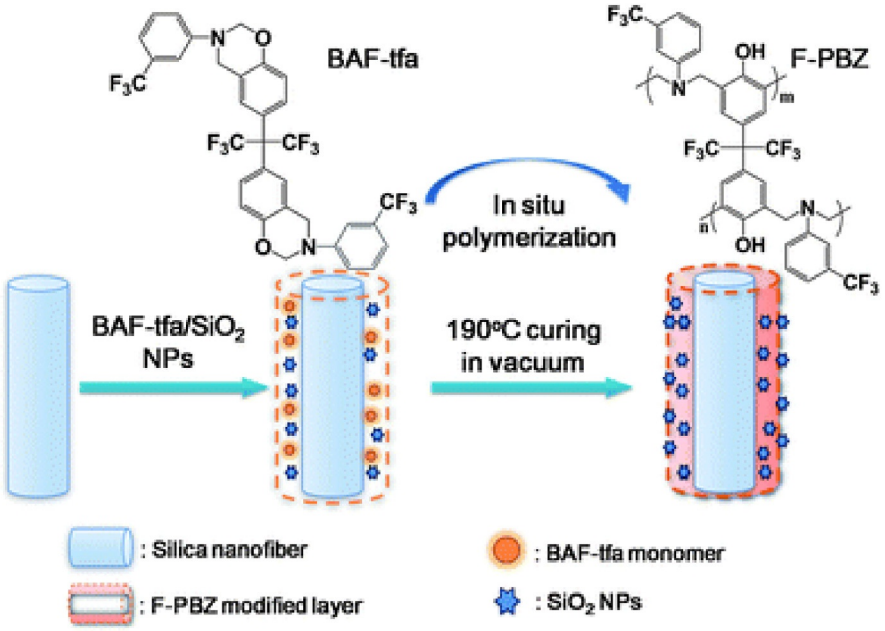

SCHEME 7 Showing the synthesis steps of poly(BAF-tfa)/SiO_2 nanoparticles (SNPs) modified silica nanofibrous membranes and the relevant formation mechanism [62].

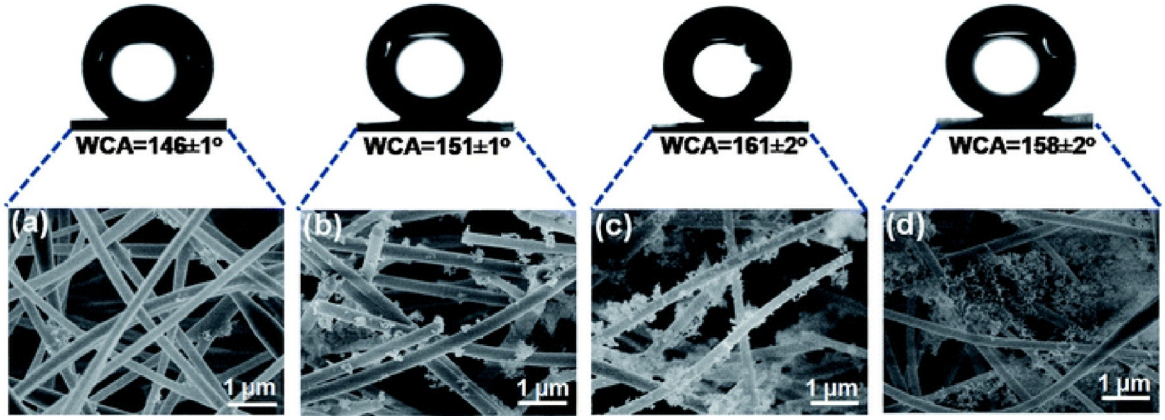

FIG. 10 FE-SEM images and the corresponding optical profiles of water droplets of (A) BAF-0.5/SNP-0.1, (B) BAF-0.5/SNP-0.5, (C) BAF-0.5/SNP-2, and (D) BAF-0.5/SNP-3 [62].

WCA of BAF-0.5/SNP (BAF-0.5 indicated the concentration of BAF-tfa was 0.5 wt% in acetone solution) increased to 161 degree after concentration of SNP was increased to 2 wt%. Fig. 10 shows those FE-SEM images of BAF-0.5 with different concentration of SNPs. As shown in FE-SEM image, 3 wt% of SNP led to aggregation of SiO_2 into clusters inside the fibers which resulted into slight decrease of WCA (158 degree ± 2 degree).

The same group also fabricated the durable superhydrophobic films by using in situ polymerization of a bifunctional fluorinated benzoxazine, 2,2-bis(3-octadecyl 1-3,4-dihydro-2*H*-1,3-benzoxazinyl)hexafluoro propane (BAF-oda) with SNPs on the glass substrate as shown in Scheme 8 [63]. As displayed in Fig. 11A, when the concentration of SNPs increased, the WCA increased to 164 degree ± 2 degree which indicates that the surface became superhydrophobic. Fig. 11B presents another important factor to investigate the ability of a surface to oppose the movement of a water droplet. Cleary, increasing contents of SNPs could lead to decreasing the WCA hysteresis for BF-3/SNP-0.8 film. (BF-3 and SNP-0.8 indicated that the concentrations of BAF-oda and SNP were 3 and 0.8 wt% in dichloromethane solution, respectively.) Fig. 12 reveals the increased surface roughness with the increasing value of topographic roughness parameter (*Ra*) and concentration of SNPs.

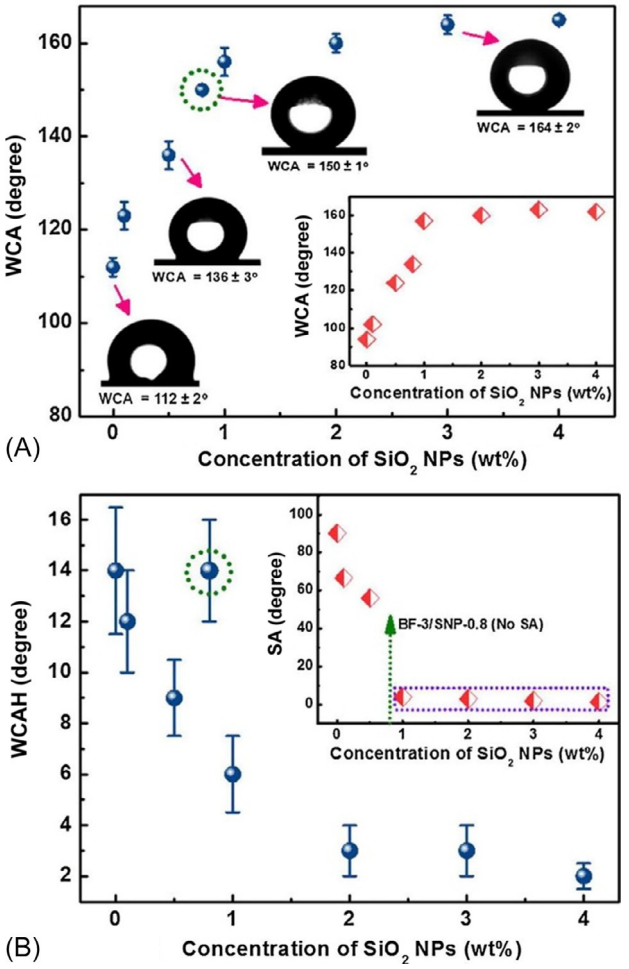

FIG. 11 (A) WCAs and the optical profiles of water droplets of various BF-3/SNP films measured as a function of SiO_2 nanoparticles (SNPs) concentration. (B) Water contact angle hysteresis (WCAHs) and sliding angles (SAs) of various BF-3/SNP films coated on glass substrate [63].

2.4.2 Polybenzoxazine/Carbon Nanotube Hybrid Superhydrophobic Surfaces

Carbon nanotube is one of the most important materials because of its potential applications, morphology, and a good performance for superhydrophobic property. Georgakilas et al. reported that the WCA of perfluorinated multiwall carbon nanotubes (MWCNTs) coated with cotton fabric

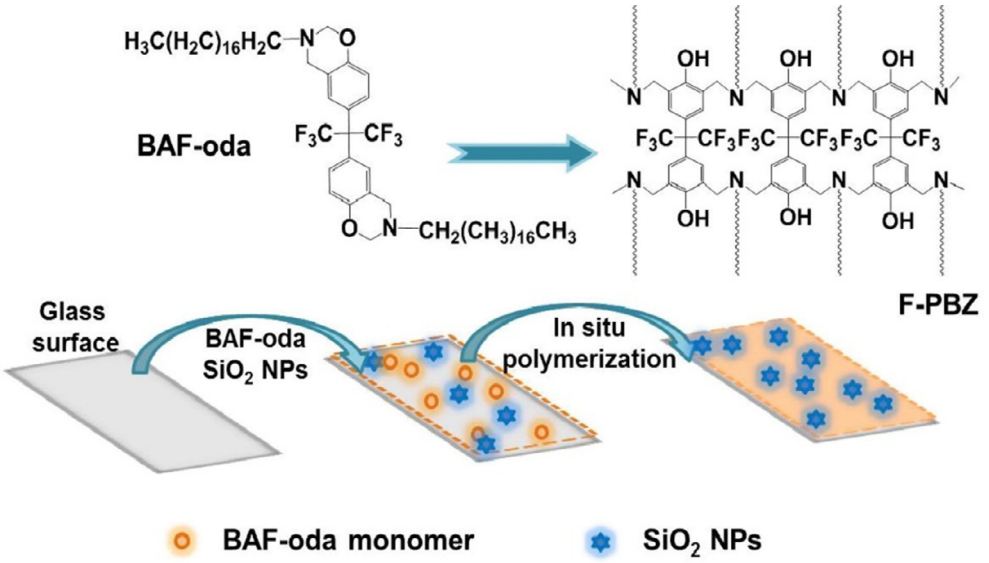

SCHEME 8 Schematic for the strategy using in situ polymerization approach to the synthesis of poly(BAF-oda)/SiO_2 nanoparticles (SNPs) coated on the glass surface [63].

was 170 degree [64]. Also, Li et al. prepared MWCNTs with aromatic azide copolymer nanocomposites coated with cotton to give WCA value more than 150 degree [65]. In 2004, Chen et al. prepared the MWCNT nanocomposites incorporating polymerized 3,3′-(((2,2-dimethylpropane-1,3-diyl)bis(oxy))bis(4,1-phenylene))bis(3,4-dihydro-2*H*-benzo[*e*][1,3]oxazine-6-carbonitrile) (MON-cy) and coated with ramie fabric as shown in Fig. 13. The WCA of (1.0 MWCNTs/1.0 MON-cy)$_{20}$ (1.0 MWCNTs and 1.0 MON-cy) indicated that the concentrations of MWCNTs and MON-cy were both 1.0 mg/mL in *N*,*N*-dimethylformamide solution (the subscript number 20 indicates the number of immersion cycles) was 152 degree ± 2 degree higher than that of (1.0 MON-cy)$_{20}$ as depicted in Fig. 14 because the MWCNTs could act as a building block [66].

Wang et al. prepared a superhydrophobic MWCNTs/poly (BA-a) nanocomposite using microwave irradiation [67]. They found that WCA value of MWCNTs/poly(BA-a) nanohybrids decreased over time, while water droplets on the surface of MWCNTs/poly(BA-a) remained as spherical structures because of the superhydrophobicity of the surface as shown in Fig. 15. SEM images show that the surface of MWCNTs/poly(BA-a) nanocomposite possessed micro-structure and binary structure, which can act as the self-cleaning lotus leaf as presented in Fig. 16. In Fig. 17A reveals that WCA values of MWCNTs/poly(BA-a) nanocomposites was decreased slightly after treatment with different organic solvents. Fig. 17B displays those MWCNTs/poly

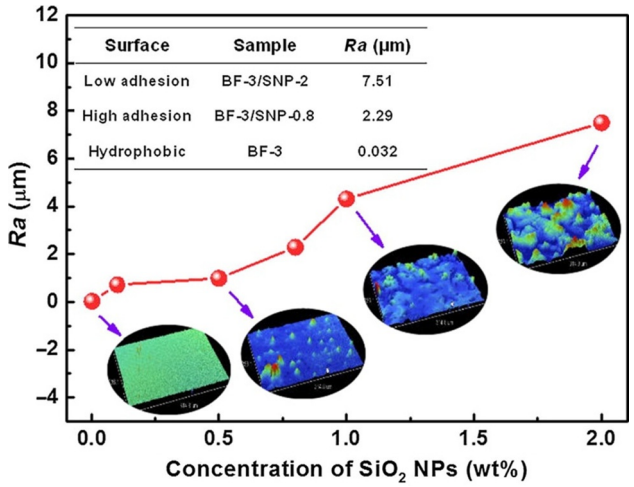

FIG. 12 The topographic roughness parameter (*Ra*) values and optical profilometry images of BF-3, BF-3/SNP-0.1, BF-3/SNP-0.5, BF-3/SNP-0.8, BF-3/SNP-1, and BF-3/SNP-2 [63].

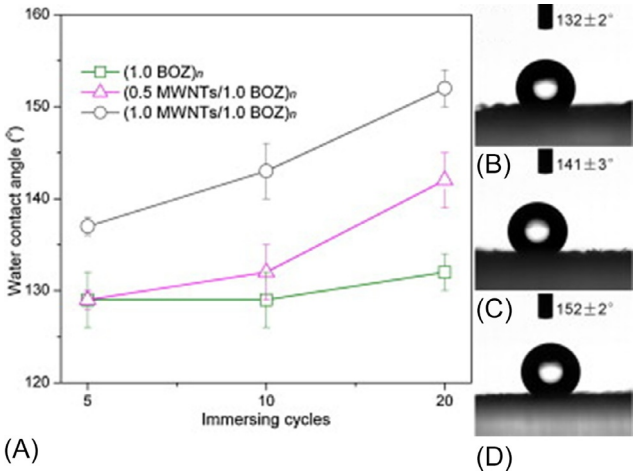

FIG. 14 (A) WCA values and photographs of water droplet of (B) (1.0 MON-cy)$_n$, (C) (0.5 MWCNTs/1.0 MON-cy)$_n$, and (D) (1.0 MWCNTs/1.0 MON-cy)$_n$ [66].

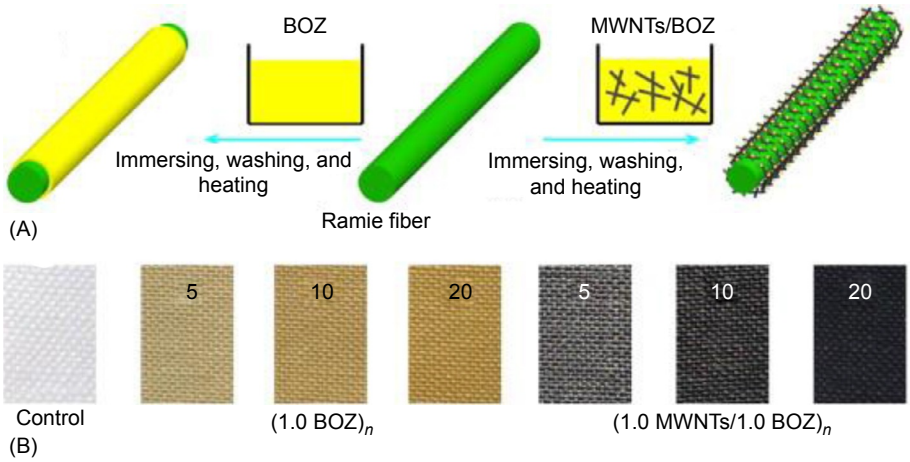

FIG. 13 (A) Schematic illustration for the construction process of poly(MON-cy) and MWCNTs/poly(MON-cy) nanocomposites on ramie fabric and (B) pictures of the pristine ramie control (1.0 MON-cy)$_n$ and (1.0 MWCNTs/1.0 MON-cy)$_n$ systems [66].

(BA-a) nanohybrids are strongly adhered to substrate with 159 degree ± 3 degree and sliding angle 5 degree.

3 CONCLUSIONS

Polybenzoxazines are a new thermosetting resin and possess many excellent properties, including near zero volumetric change after polymerization, low melting viscosity for benzoxazine monomer, high glass transition temperature, high thermal stability, low water absorption, excellent dielectric properties, and good mechanical properties. The studies of the surface properties for polybenzoxazines, however, are issued rarely. In this chapter, we have reviewed the studies

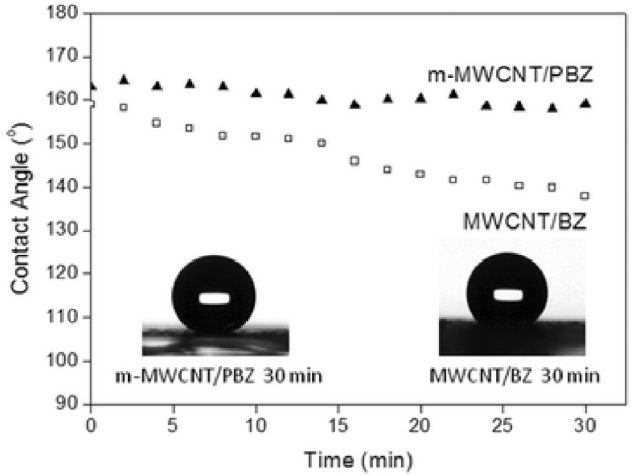

FIG. 15 Time dependence of the WCAs of the MWCNTs/(BA-a) and m-MWCNTs/poly(BA-a) (polymerized by microwave) nanocomposites [67].

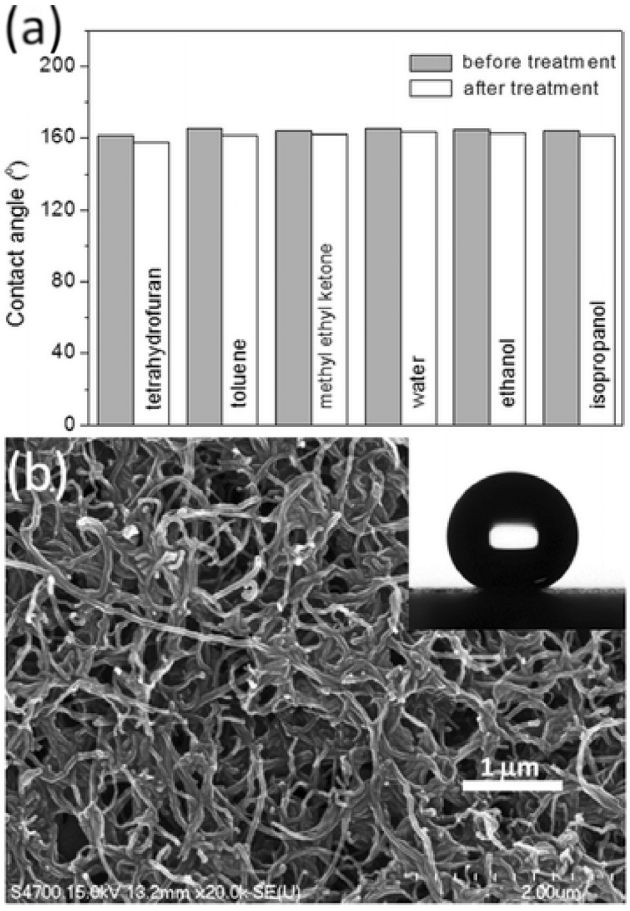

FIG. 17 (A) Durability of the superhydrophobic films after treatment with organic solvents and (B) SEM images of m-MWCNTs/poly(BA-a) (polymerized by microwave) nanocomposites after performing the tape test [67].

FIG. 16 (A) Profile of the water drop on the m-MWCNT–PBZ superhydrophobic surface. (B) Large-area SEM image of the m-MWCNT–PBZ superhydrophobic surface. (C) Enlarged view of a micro-island in (B). (D) SEM image of the lower surface of the superhydrophobic film [67].

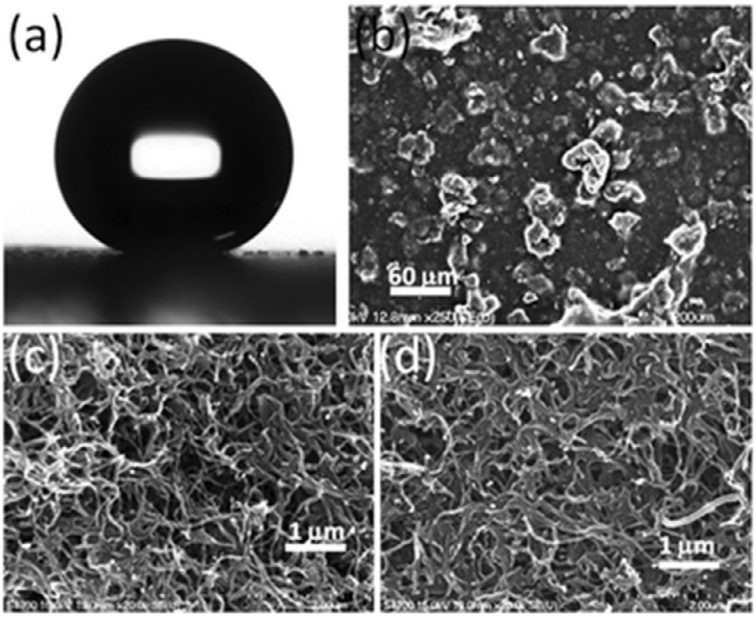

of surface properties such as the surface free energy, anti-sticking application in nanoimprint technology, tunable surface properties, durable resistance enhancements, and superhydrophobic properties.

REFERENCES

[1] F. Ciardelli, M. Aglietto, L.M. di Mirabello, E. Passaglia, S. Giancristoforo, V. Castelvetro, G. Ruggeri, New fluorinated acrylic polymers for improving weather ability of building stone materials, Prog. Org. Coat. 32 (1997) 43–50.

[2] L. Klinger, J.R. Griffith, C.J.N. Rall, Fluoropolymer barriers to stress corrosion in optical fibers, Org. Coat. Appl. Polym. Sci. Proc. 48 (1983) 407–411.

[3] C. Bonardi, Fluoroacrylic telomers and their use as hydrofuge and oleofuge products on diverse substrates, Eur. Pat Appl. EP 426530; 1991.

[4] Y. Matsumoto, K. Yoshida, M. Ishida, A novel deposition technique for fluorocarbon films and its applications for bulk- and surface-micromachined devices, Sens. Actuators 66 (1998) 308–314.

[5] M.H. Anderson, C.S. Lyons, B.D. Wigness, Implantable catheters with non-adherent contacting polymer surfaces, U.S. Patent 4536179; 1985.

[6] S.R. Coulson, I. Woodward, J.P.S. Badyal, S.A. Brewer, C. Willis, Super-repellent composite fluoropolymer surfaces, J. Phys. Chem. B 104 (2000) 8836–8840.

[7] M. Jin, X. Feng, J. Xi, J. Zhai, K. Cho, L. Feng, L. Jiang, Super-hydrophobic PDMS surface with ultra-low adhesive force, Macromol. Rapid Commun. 26 (2005) 1805–1809.

[8] L. Feng, Z. Zhang, Z. Mai, Y. Ma, B. Liu, L. Jiang, et al., A super-hydrophobic and super-lyophilic coating mesh film for the separation of oil and water, Angew. Chem. Int. Ed. 43 (2004) 2012–2014.

[9] H. Hillborg, N. Tomczak, A. Olah, H. Schonherr, G.J. Vancso, Nano-scale hydrophobic recovery: a chemical force microscopy study of uv/ozone-treated cross-linked poly(dimethylsiloxane), Langmuir 20 (2004) 785–794.

[10] S. Wu, Contact angles of liquids on solid polymers, in: S. Wu (Ed.), Polymer Interface and Adhesion, Marcel Dekker, New York, NY, 1982, pp. 133–168.

[11] D.P. Carlson, W. Schmiegel, Fluoropolymers, organic, in: W. Gerhartz (Ed.), Ullmann's Encyclopedia of Industrial Chemistry, fifth ed., VCH Verlagsgesellschaft, Weinheim, 1988, pp. 393–429.

[12] H. Kobayashi, M.J. Owen, Surface properties of fluorosilicones, Trends Polym. Sci. 3 (1995) 330–335.

[13] D.L. Schmidt, C.E. Coburn, B.M. DeKoven, G.E. Potter, G. F. Meyers, D.A. Fischer, Role of the product in the transformation of a catalyst to its active state, Nature 368 (1994) 41–45.

[14] W.A. Zisman, Influence of constitution on adhesion, Ind. Eng. Chem. 55 (1963) 18–38.

[15] F.M. Fowkes, Determination of interfacial tensions, contact angles, and dispersion forces in surfaces by assuming additivity of intermolecular interactions in surfaces, J. Phys. Chem. 66 (1962) 382.

[16] C.J. Drummond, G. Georgaklis, D.Y.C. Chan, Fluorocarbons: surface free energies and van der Waals interaction, Langmuir 11 (1996) 2617–2621.

[17] J. Hopken, M. Moller, Low-surface-energy polystyrene, Macromolecules 25 (1992) 1461–1467.

[18] D.K. Owens, R.C. Wendt, Estimation of the surface free energy of polymers, J. Appl. Polym. Sci. 13 (1969) 1741–1747.

[19] D.H. Kaelble, A reinterpretation of organic liquid-polytetrafluoroethylene surface interactions, J. Adhes. 2 (1970) 50–60.

[20] K. Ma, T. Chung, R.J. Good, Surface energy of thermotropic liquid crystalline polyesters and polyesteramide, J. Polym. Sci. B Polym. Phys. 36 (1998) 2327–2337.

[21] C.J. van Oss, M.K. Chaudhury, R.J. Good, Interfacial Lifshitz-van der Waals and polar interactions in macroscopic systems, Chem. Rev. 88 (1988) 927–941.

[22] C.J. van Oss, L. Ju, M.K. Chaudhury, R.J. Good, Estimation of the polar parameters of the surface tension of liquids by contact angle measurements on gels, J. Colloid Interface Sci. 128 (1989) 313–319.

[23] C.J. van Oss, R.F. Giese Jr., R.J. Good, Reevaluation of the surface tension components and parameters of polyacetylene from contact angles of liquids, Langmuir 6 (1990) 1711–1713.

[24] R.J. Good, C.J. van Oss, The modern theory of contact angles and the hydrogen bond components of surface energies, in: M.E. Schrader, G.I. Loeb (Eds.), Modern Approaches to Wettability: Theory and Applications, Plenum Press, New York, NY, 1992, pp. 1–27.

[25] M.J. Owen, Low surface energy inorganic polymers, Comments Inorg. Chem. 7 (1988) 195–213.

[26] J. Tsibouklis, T.G. Nevell, Ultra-low surface energy polymers: the molecular design requirements, Adv. Mater. 15 (2003) 647–650.

[27] K.X. Ma, T.S. Chung, Effect of $-C(CF_3)_2$ on the surface energy of main-chain liquid crystalline and crystalline polymers, J. Phys. Chem. B 105 (2001) 4145–4150.

[28] T. Sun, G. Wang, L. Feng, B. Liu, Y. Ma, L. Jiang, D. Zhu, Reversible switching between superhydrophilicity and superhydrophobicity, Angew. Chem. Int. Ed. 43 (2004) 357–360.

[29] (a) X. Ning, H. Ishida, Phenolic materials via ring-opening polymerization: synthesis and characterization of bisphenol-A based benzoxazines and their polymers, J. Polym. Sci. A Polym. Chem. 32 (1994) 1121–1129; (b)Y.X. Wang, H. Ishida, Cationic ring-opening polymerization of benzoxazines, Polymer 40 (1999) 4563–4570; (c)J.A. Macko, H. Ishida, Structural effects of phenols on the photooxidative degradation of polybenzoxazines, Polymer 42 (2001) 227–240.

[30] H. Ishida, D.J. Allen, Physical and mechanical characterization of near-zero shrinkage polybenzoxazines, J. Polym. Sci. B Polym. Phys. 34 (1996) 1019–1030.

[31] W. Ma, H. Wu, Y. Hiqaki, H. Otsuka, A. Takahara, A "non-sticky" superhydrophobic surface prepared by self-assembly of fluoroalkyl phosphonic acid on a hierarchically micro/nanostructured alumina gel film, Chem. Commun. 48 (2012) 6824–6826.

[32] M. Ma, R.M. Hill, J.L. Lowery, S.V. Fridrikh, G.C. Rutledge, Electrospun poly(styrene-block-dimethylsiloxane) block copolymer fibers exhibiting superhydrophobicity, Langmuir 21 (2005) 5549–5554.

[33] T. Kamegawa, Y. Shimizu, H. Yamashita, Superhydrophobic surfaces with photocatalytic self-cleaning properties by nanocomposite coating of TiO_2 and polytetrafluoroethylene, Adv. Mater. 24 (2012) 3697–3700.

[34] D.E. Weibel, A.F. Michels, A.F. Feil, L. Amaral, S.R. Teixeira, F. Horowitz, Adjustable hydrophobicity of Al substrates by chemical surface functionalization of nano/microstructures, J. Phys. Chem. C 114 (2010) 13219–13225.

[35] C.F. Wang, Y.C. Su, S.W. Kuo, C.F. Huang, Y.C. Sheen, F.C. Chang, Low-surface-free-energy materials based on polybenzoxazines, Angew. Chem. Int. Ed. 45 (2006) 2248–2251.

[36] L. Qu, Z. Xin, Preparation and surface properties of novel low surface free energy fluorinated silane-functional polybenzoxazine films, Langmuir 27 (2011) 8365–8370.

[37] L. Juan, J. Liu, X. Lu, Z. Xin, C. Zhou, Synthesis and surface properties of low surface free energy silane-functional polybenzoxazine films, Langmuir 29 (2013) 411–416.
[38] T.H. Kao, J.K. Chen, C.C. Cheng, C.I. Su, C.F. Chang, Low-surface-free-energy polybenzoxazine/polyacrylonitrile fibers for bionon-fouling membrane, Polymer 54 (2013) 258–268.
[39] S.W. Kuo, F.C. Chang, POSS related polymer nanocomposites, Prog. Polym. Sci. 36 (2011) 1649–1696.
[40] Y.C. Wu, S.W. Kuo, Synthesis and characterization of polyhedral oligomeric silsesquioxane (POSS) with multifunctional benzoxazine groups through click chemistry, Polymer 51 (2010) 3948–3955.
[41] C.F. Wang, S.F. Chiou, F.H. Ko, J.K. Chen, C.T. Chou, C.F. Huang, F. C. Chang, Polybenzoxazine as a mold-release agent for nanoimprint lithography, Langmuir 23 (2007) 5868–5871.
[42] Y.S. Wang, C.H. Hung, C.H. Lee, H.W. Hung, Polybenzoxazine a non-fluorinated polymer for anti-adhesion surface treatment of moulds, Int. J. Nanomanuf. 9 (2013) 1–9.
[43] Q. Fu, G.V. Rama Rao, S.B. Basame, D.J. Keller, K. Artyushkova, J. E. Fulghum, G.P. López, Reversible control of free energy and topography of nanostructured surfaces, J. Am. Chem. Soc. 126 (2004) 8904–8905.
[44] S.J. Choi, K.Y. Suh, H.H. Lee, Direct UV-replica molding of biomimetic hierarchical structure for selective wetting, J. Am. Chem. Soc. 130 (2008) 6312–6313.
[45] R. Rosario, D. Gust, M. Hayes, F. Jahnke, J. Springer, A.A. Garcia, Photon-modulated wettability changes on spiropyran-coated surfaces, Langmuir 18 (2002) 8062–8069.
[46] X. Feng, L. Feng, M. Jin, J. Zhai, L. Jiang, D. Zhu, Reversible superhydrophobicity to super-hydrophilicity transition of aligned ZnO nanorod films, J. Am. Chem. Soc. 126 (2004) 62–63.
[47] W. Zhang, X. Lu, Z. Xin, C. Zhou, J. Liu, Fluorine-free superhydrophobic/hydrophobic polybenzoxazine/TiO_2 films with excellent thermal stability and reversible wettability, RSC Adv. 5 (2015) 55513–55519.
[48] S. Minko, M. Müller, M. Motornov, M. Nitschke, K. Grundke, M. Stamm, Two-level structured self-adaptive surfaces with reversibly tunable properties, J. Am. Chem. Soc. 125 (2003) 3896–3900.
[49] T.N. Krupenkin, J.A. Taylor, T.M. Schneider, S. Yang, From rolling ball to complete wetting: the dynamic tuning of liquids on nanostructured surfaces, Langmuir 20 (2004) 3824–3827.
[50] M.G. Mohamed, W.C. Su, Y.C. Lin, C.F. Wang, J.K. Chen, K. U. Jeong, S.W. Kuo, Azopyridine-functionalized benzoxazine with Zn $(ClO_4)_2$ form high-performance polybenzoxazine stabilized through metal–ligand coordination, RSC Adv. 4 (2014) 50373–50385.
[51] M.G. Mohamed, C.H. Hsiao, K.C. Hsu, F.H. Lu, H.K. Shih, S.W. Kuo, Supramolecular functionalized polybenzoxazines from azobenzene carboxylic acid/azobenzene pyridine complexes: synthesis, surface properties, and specific interactions, RSC Adv. 5 (2015) 12763–12772.
[52] M.G. Mohamed, C.H. Hsiao, F. Luo, L. Dai, S.W. Kuo, Multifunctional polybenzoxazine nanocomposites containing photoresponsive azobenzene units, catalytic carboxylic acid groups, and pyrene units capable of dispersing carbon nanotubes, RSC Adv. 5 (2015) 45201–45212.
[53] W.C. Su, S.W. Kuo, Reversible surface properties of polybenzoxazine/silica nanocomposites thin films, J. Nanomater. 97 (2013) 1–12.
[54] Y. Lu, S. Sathasivam, J. Song, C.R. Crick, C.J. Carmalt, I.P. Parkin, Robust self-cleaning surfaces that function when exposed to either air or oil, Science 347 (2015) 1132–1135.
[55] C. Dai, N. Liu, Y. Cao, Y. Chen, F. Lu, L. Feng, Fast formation of superhydrophobic octadecylphosphonic acid (ODPA) coating for self-cleaning and oil/water separation, Soft Matter 10 (2014) 8116–8121.
[56] X. Hong, X. Gao, L. Jiang, Application of superhydrophobic surface with high adhesive force in no lost transport of superparamagnetic microdroplet, J. Am. Chem. Soc. 129 (2007) 1478–1479.
[57] X. Gao, L. Jiang, Biophysics: water-repellent legs of water striders, Nature 432 (2004) 36.
[58] R.N. Wenzel, Resistance of solid surfaces to wetting by water, Ind. Eng. Chem. 28 (1936) 988–994.
[59] A.B.C. Cassie, S. Baxter, Wettability of porous surfaces, Trans. Faraday Soc. 40 (1944) 546–551.
[60] C.S. Liao, C.F. Wang, H.C. Lin, H.Y. Chou, F.C. Chang, Fabrication of patterned superhydrophobic polybenzoxazine hybrid surfaces, Langmuir 25 (2009) 3359–3362.
[61] C.F. Wang, Y.T. Wang, P.H. Tung, S.W. Kuo, C.H. Lin, Y.C. Sheen, F.C. Chang, Stable superhydrophobic polybenzoxazine surfaces over a wide pH range, Langmuir 22 (2006) 8289–8292.
[62] L. Yang, A. Raza, Y. Si, X. Mao, Y. Shang, B. Ding, S.S. Al-Deyab, Synthesis of superhydrophobic silica nanofibrous membranes with robust thermal stability and flexibility via in situ polymerization, Nanoscale 4 (2012) 6581–6587.
[63] A. Raza, Y. Si, B. Ding, J. Yu, G. Sun, Fabrication of superhydrophobic films with robust adhesion and dual pinning state via in situ polymerization, J. Colloid Interface Sci. 395 (2013) 256–262.
[64] V. Georgakilas, A.B. Bourlinos, R. Zboril, C. Trapalis, Synthesis, characterization and aspects of superhydrophobic functionalized carbon nanotubes, Chem. Mater. 20 (2008) 2884–2886.
[65] G. Li, H. Wang, H. Zheng, R. Bai, A facile approach for the fabrication of highly stable superhydrophobic cotton fabric with multi-walled carbon nanotubes-azide polymer composites, Langmuir 26 (2010) 7529–7534.
[66] T. Zhang, H. Yan, Z. Fang, E. Yuping, T. Wu, F. Chen, Superhydrophobic and conductive properties of carbon nanotubes/polybenzoxazine nanocomposites coated ramie fabric prepared by solution-immersion process, Appl. Surf. Sci. 309 (2014) 218–224.
[67] C.F. Wang, H.Y. Chen, S.W. Kuo, Y.S. Lai, P.F. Yang, Rapid, low temperature microwave synthesis of durable, superhydrophobic carbon nanotube–polybenzoxazine nanocomposites, RSC Adv. 3 (2013) 9764–9769.